Biomaterials xxx (2013) 1–8

Contents lists available at SciVerse ScienceDirect

Biomaterials

journal homepage: www.elsevier.com/locate/biomaterials

Dynamic tissue engineering scaffolds with stimuli-responsive macroporosity formation

Li-Hsin Han [a], Janice H. Lai [b], Stephanie Yu [c], Fan Yang [a,d,*]

[a] Department of Orthopaedic Surgery, Stanford University, Stanford, CA 94305, USA
[b] Department of Mechanical Engineering, Stanford University, Stanford, CA 94305, USA
[c] Program in Human Biology, Stanford University, Stanford, CA 94305, USA
[d] Department of Bioengineering, Stanford University, Stanford, CA 94305, USA

ARTICLE INFO

Article history:
Received 6 February 2013
Accepted 19 February 2013
Available online xxx

Keywords:
Porogen
Scaffold
Macroporosity
Hydrogels
Pore formation

ABSTRACT

Macropores in tissue engineering scaffolds provide space for vascularization, cell-proliferation and cellular interactions, and is crucial for successful tissue regeneration. Modulating the size and density of macropores may promote desirable cellular processes at different stages of tissue development. Most current techniques for fabricating macroporous scaffolds produce fixed macroporosity and do not allow the control of porosity during cell culture. Most macropore-forming techniques also involve non-physiological conditions, such that cells can only be seeded in a post-fabrication process, which often leads to low cell seeding efficiency and uneven cell distribution. Here we report a process to create dynamic hydrogels as tissue engineering scaffolds with tunable macroporosity using stimuli-responsive porogens of gelatin, alginate and hyaluronic acid, which degrade in response to specific stimuli including temperature, chelating and enzymatic digestion, respectively. SEM imaging confirmed sequential pore formation in response to sequential stimulations: 37 °C on day 0, EDTA on day 7, and hyaluronidase on day 14. Bovine chondrocytes were encapsulated in the Alg porogen, which served as cell-delivery vehicles, and changes in cell viability, proliferation and tissue formation during sequential stimuli treatments were evaluated. Our results showed effective cell release from Alg porogen with high cell viability and markedly increased cell proliferation and spreading throughout the 3D hydrogels. Dynamic pore formation also led to significantly enhanced type II and X collagen production by chondrocytes. This platform provides a valuable tool to create stimuli-responsive scaffolds with dynamic macroporosity for a broad range of tissue engineering applications, and may also be used for fundamental studies to examine cell responses to dynamic niche properties.

© 2013 Elsevier Ltd. All rights reserved.

1. Introduction

Culturing cells in three dimensions (3D) has been shown to induce cellular behavior that more closely mimics in vivo scenario [1–3]. Hydrogels are attractive scaffolds for 3D cell culture and tissue engineering due to their tissue-like water content, injectability, and tunable properties [4–6]. Extensive efforts have been made to control various cues of hydrogels including biochemical, physical and topographical cues, for the purpose of promoting desirable cellular processes and subsequent tissue formation [7]. Macropores within hydrogels are important microstructures that promote tissue formation by facilitating diffusion, cell proliferation, migration, and extracellular matrix (ECM) production.

Various platforms have been developed to create macroporous structures within 3D tissue engineering scaffolds, including 3D printing [8], stereolithography [9–11], polymer phase separation, lyophilizing [12,13], gas foaming [14], and porogen leaching using salt, emulsified droplets, or polymeric microspheres [15–19]. Despite the breath of available technology for creating macroporosity in 3D scaffolds, several challenges remain before they can be applied broadly for tissue engineering applications. First, most methods developed so far only allow fabricating scaffolds with preformed, fixed porosity. However, different macropore size and density may be desirable at different stages of tissue development. While low porosity is preferred for initial structural stability and protection of transplanted cells, increased porosity over time is important to accommodate efficient blood vessel ingrowth, nutrients diffusion, as well as creating space for cell proliferation and matrix production [20,21]. Scaffolds made from biodegradable polymers [22–24] allow increasing porosity over time, but

* Corresponding author. Department of Bioengineering, Stanford University, Stanford, CA 94305, USA.
E-mail address: fanyang@stanford.edu (F. Yang).

0142-9612/$ – see front matter © 2013 Elsevier Ltd. All rights reserved.
http://dx.doi.org/10.1016/j.biomaterials.2013.02.051

Please cite this article in press as: Han L-H, et al., Dynamic tissue engineering scaffolds with stimuli-responsive macroporosity formation, Biomaterials (2013), http://dx.doi.org/10.1016/j.biomaterials.2013.02.051

lack direct control over the timing and degree of macropore-formation in accordance with the stages of tissue formation. Second, current methods to fabricate macroporous scaffolds often involve fabrication conditions that are too harsh for cells to survive, such as excess heat [16,17], extreme pressure [12,14], non-physiological salt concentration [15], or use of organic solvents [16,17]. Therefore, cells can only be seeded onto the prefabricated macroporous scaffolds, which often leads to low cell seeding efficiency and non-uniform distribution. More recent work has reported co-encapsulating of cells and non-cytotoxic porogens, which allowed more controlled cell distribution [18,19]. However, these platforms do not allow dynamic macropore formation and often lead to limited cell migration due to the trapping by hydrogels.

To overcome the aforementioned limitations, here we aim to develop a process that allows dynamic formation of macropores in cell-laden hydrogels in a stimuli-responsive manner (Fig. 1). We hypothesize that embedding multiple types of stimuli-responsive porogens in hydrogel scaffolds will lead to sequential formation of macropores within hydrogels, and such sequential pore formation will enhance cell proliferation and ECM production over time. To test our hypotheses, we fabricated type-B gelatin hydrogels containing three types of microspherical porogens based on type-A gelatin (Gel-A), alginate (Alg), and glycidyl-methacrylated hyaluronic acid (GMHA) (Fig. 1A), which have been widely used as biomaterials for tissue engineering applications [25–28]. These porogens degrade in response to specific stimuli including temperature (37 °C), small-molecule chelating, and enzymatic digestion, respectively. The potential of using such porogens as cell-delivery vehicles was examined by encapsulating neonatal bovine chondrocytes (BACs) in alginate-based porogens to offer cells initial protection, while releasing them in a stimuli-responsive manner. Hydrogels containing multiple porogens were exposed to multiple stimuli in a stage-wise manner to promote nutrient diffusion (Fig. 1B), release encapsulated cells into macroporous space (Fig. 1C), and create space for further cell proliferation and tissue formation (Fig. 1D). Scaffold morphology was examined using scanning electron microscopy and fluorescence imaging. Cell viability, proliferation and tissue formation during sequential stimuli treatments were also evaluated at multiple time points.

2. Materials and methods

2.1. Materials

Type-A and type-B gelatin, triethylamine, glycidyl methacrylate, alginate sodium salt (medium molecular weight), Fluorescein-5-EX N-hydroxysuccinimide ester (NHS-fluorescein), hyaluronidase, lecithin surfactant, and paraformaldehyde were purchased from Sigma–Aldrich (St. Louis, MO). Hyaluronic acid sodium salt was purchased from Lifecore Biomedical (Chaska, MN). 4-(2-hydroxyethoxy) phenyl-(2-hydroxy-2-propyl) ketone, or Irgacure 2959 (Ir2959), was supplied from Ciba Specialty Chemistry (Basel, Switzerland). Ethylenediaminetetraacetic acid (EDTA) and disodium citrate were purchased from Fisher Scientific International (Hampton, NH). All materials were used as received.

2.2. Synthesis of methacrylated Type-B gelatin (GelB-MA)

To make photocrosslinkable gelatin hydrogels, methacrylate end groups were introduced onto Type B gelatin as previously reported [25]. Briefly, type-B gelatin (GelB) (10 g) was dissolved in 100 mL DPBS under 50 °C, and methacrylic anhydride

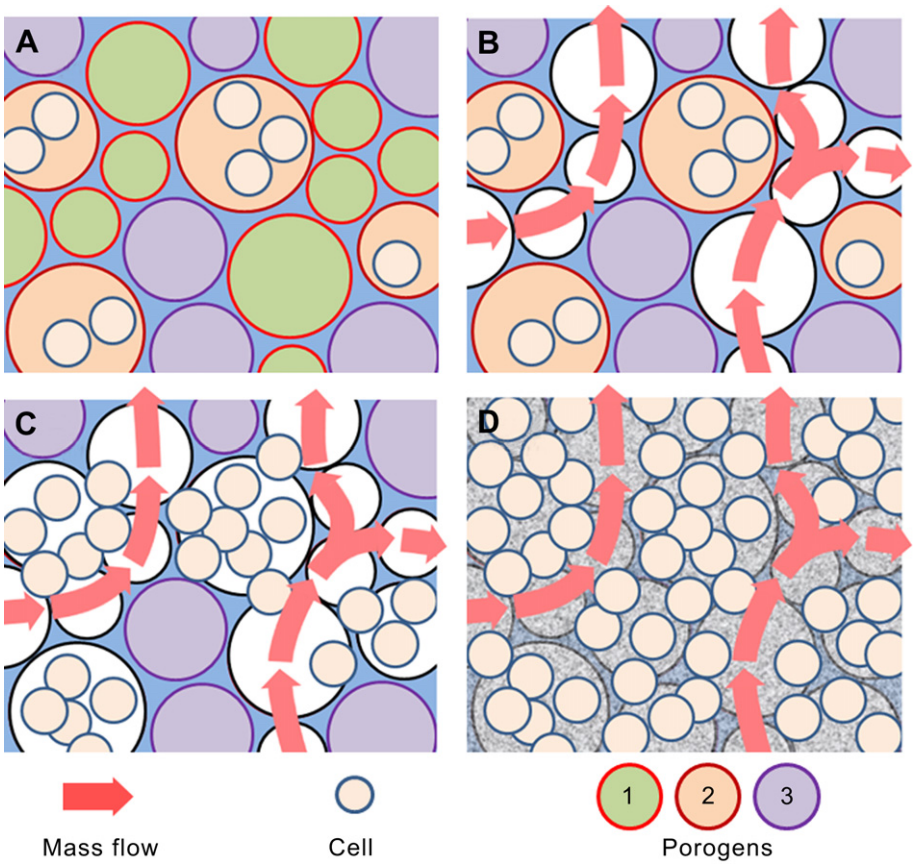

Fig. 1. Schematic of sequential macropore formation in cell-laden hydrogels using stimuli-responsive porogens. Porogens 1, 2 and 3 are made of type-A gelatin, alginate, and hyaluronic acid respectively. (A) Forming cell-laden hydrogels by mixing three different types of porogens in 3D gelatin solution, with cell pre-encapsulated in porogen 2; (B) Removing porogen 1 to facilitate mass transfer; (C) Removing porogen 2 to release cells and facilitate cell proliferation; and (D) removing porogen 3 to promote further cell proliferation and deposition of extracellular matrix.

Please cite this article in press as: Han L-H, et al., Dynamic tissue engineering scaffolds with stimuli-responsive macroporosity formation, Biomaterials (2013), http://dx.doi.org/10.1016/j.biomaterials.2013.02.051

(20 mL) was slowly added under constant stirring at 1000 rpm. The reaction continued for 3 h at 50 °C. Crude product of GelB-MA was extracted by dripping the solution into acetone (3L), which precipitated GelB-MA and removed excessive methacrylic anhydride and by products. The GelB-MA was purified by dialysis in DI water, lyophilized, and stored at −20 °C until use.

2.3. Synthesis of methacrylated hyaluronic acid (GMHA)

Methacrylated hyaluronic acid (HA) was synthesized as previously reported [28]. In brief, hyaluronic acid (HA) sodium salt (5 g, average M_W = 65,000) was dissolved in DI water (180 mL). Triethylamine (37.5 mL) and glycidyl methacrylate (35.5 mL) were added to methacrylate the hydroxyl groups of HA. The solution was stirred overnight at room temperature. GMHA was collected by precipitating the solution in 20-fold volume of acetone in the presence of NaCl crystals (10 g). The GMHA was purified by dialysis in DI water, lyophilized, and stored at −20 °C until use.

2.4. Fabricating stimuli-responsive porogens

GelA (10% wt/v) was dissolved in DPBS at 40 °C to form GelA solution. Lecithin was dissolved in olive oil to a final concentration of 3% wt/v. To form gelatin microparticles, the olive oil containing lecithin (15 mL) was heated to 40 °C and stirred at 700 rpm in a 20 mL beaker, and GelA solution (3 mL) was added drop-wise into the stirred olive oil to form a water-in-oil-phase emulsion. After 10 min, the stirring speed was lowered to 200 rpm, and the emulsion was cooled to 4 °C by ice bath for 30 min. The cooling led to formation of GelA microparticles in olive oil. The GelA microparticles were collected by gentle centrifuge, washed five times by PBS, and stored at 4 °C. To fabricate GMHA porogens, GMHA precursor solution was prepared by dissolving GMHA (10 wt%) and Ir2959 (0.05 wt%) in PBS. The olive oil with lecithin (15 mL) was added to a 20 mL beaker and stirred at 700 rpm, and the GMHA hydrogel precursor (3 mL) was added by drops into the stirred olive oil to form a water-in-oil-phase emulsion. To create GMHA hydrogel microparticles for porogen, the emulsion was exposed to ultraviolet light (365 nm, 4 mW/cm^2) for 10 min under stirring, which polymerized GMHA and turned the emulsified droplets into hydrogel microparticles. The microparticles were collected and washed five times by PBS before stored at 5 °C. To prepare porogen from alginate, alginate dissolved in DPBS (2% w/v, 10 mL) was added drop-wise into the olive oil containing lecithin (30 mL) under constant stirring at 1000 rpm for 10 min to form a water-in-oil emulsion. The emulsion was then rapidly mixed with aqueous solution of CaCl2 (1% w/v, 40 mL), which crosslinked alginate molecules into spherical microparticles. The Alg-Ca microparticles were washed five times by PBS and stored at 5 °C until use.

2.5. Fabricating hydrogels with multiple stimuli-responsive porogens

GelB-MA hydrogel precursor for the non-dissolving part of scaffold was prepared by dissolving GelB-MA (20 wt%) and Ir2959 (0.05 wt%) in PBS. Each type of the porogen microparticles (GelA, Alg-Ca, or GMHA) were rinsed three times by the GelB-MA precursor, and concentrated by removing excess GelB-MA precursor through a 70 μm nylon mesh, forming a porogen paste. To prepare the dynamic scaffolds with one type of porogen (mono-porogen scaffold), each porogen paste was molded (3 mm thick, 5.8 mm in diameter) and exposed to ultraviolet (UV) light (365 nm and 4 mW/cm^2) for 5 min, which crosslinked GelB-MA and turned the porogen paste into a hydrogel packed with porogen microparticles. To create a scaffold that contains three types of porogens (tri-porogen scaffold), the porogen pastes were mixed by equal volumes and was crosslinked following the same molding and exposure steps.

2.6. Stimuli-responsive pore-formation

2.6.1. Pore-formation in mono-porogen scaffolds

To study the effects of individual type of porogen (GelA, Alg-Ca, and GMHA) on macropore formation, hydrogels containing mono-porogens were treated by different stimuli. The scaffold with GelA porogen was incubated in PBS overnight at 37 °C. The scaffold with Alg-Ca porogen was incubated for 2 h in a DPBS solution of 8 mM EDTA (8 mM) and disodium citrate (12 mM). The scaffold with GMHA porogen was incubated at 37 °C for 3 h in PBS with hyaluronidase (300 units/mL), which cleaved the β-N-acetylhexosamine-[1→4] glycosidic bonds in hyaluronic acid [29]. After each treatment, the scaffold was rinsed by DI water five times and fluorescently labeled by NHS-fluorescein (15 mg/mL in PBS). Scaffold morphology after the porogen removal was examined using a Zeiss fluorescence microscope and a Hitachi S-3400N variable pressure scanning electron microscope (VP-SEM).

2.6.2. Sequential pore-formation in tri-porogen scaffolds

Tri-porogen scaffolds were prepared and treated by the stimuli in a sequential manner: incubation in 37 °C PBS overnight, incubation in EDTA/disodium citrate solution for 2 h, and incubation in 37 °C hyaluronidase solution for 3 h. Samples were collected after each treatment and scaffold morphology was examined using VP-SEM.

2.6.3. Characterizing scaffold morphology using scanning electron microscopy

To prepare for SEM imaging, all samples were incubated in PBS at 37 °C overnight and rinsed by DI water. The hydrated samples were then placed into the SEM chamber and gradually cooled from room temperature to −25 °C as the chamber pressure reduced from 1 atm to 50 Pa, following a P/T curve at which water maintains liquid phase. The samples were imaged under electron-beam intensity at 15 kV and a working distance around 7 mm.

2.7. Cell activities in the scaffolds with dynamic pore-formation

2.7.1. Harvesting and culturing bovine articular chondrocytes (BAC)

Hyaline articular cartilage was dissected from the femoropatellar groove of two stifle joints from a three-day old calf (Research 87, Marlborough, MA). The cartilage was sliced into thin pieces and digested in high glucose DMEM containing 1 mg/mL of collagenase (type II and type IV), 100 U/mL penicillin and 0.1 mg/mL streptomycin for 48 h at 37 °C. Digested suspension was filtered through a 70 μm nylon mesh, washed in DPBS and centrifuged at 460 g for 15 min for three times before plating. The bovine articular chondrocytes (BACs) were expanded in chondrocyte culture medium containing high glucose DMEM, 10% (v/v) fetal bovine serum, 10 mM HEPES, 0.1 mM nonessential amino acid, 0.4 mM L-proline, 50 μg/mL ascorbic acid, 1 mM sodium pyruvate, 100 U/mL penicillin, and 0.1 mg/mL streptomycin. Passage 2 BACs were used for subsequent experiments.

2.7.2. Encapsulating BACs in Alg-Ca porogens

Passage 2 BACs were suspended at 5 million cells per mL in DMEM containing 2% (w/v) sodium alginate. To encapsulate BACs in Alg-Ca porogens, alginate solution containing BACs was ejected at 0.5 mL/min using a syringe pump into sterile salt solution containing CaCl2 (1% w/v) and NaCl (0.9% w/v) under stirring (500 rpm). The resulting cell-containing Alg-Ca porogens were incubated in chondrocyte culture medium at 37 °C for 1 day before being incorporated into the tri-porogen scaffolds.

2.7.3. Dynamic macropore formation and controlled delivery of BACs in tri-porogen scaffolds

Three types of porogens were mixed together by equal volume, molded and exposed to UV light (365 nm, 4 mW/cm^2) for 5 min. All samples were divided into 3 groups (n = 16/group) with exposure to stimuli for single, dual, or tri-porogen removal. All groups received the removal of GelA porogen by overnight incubation at 37 °C at day 0. Group 2 received additional Alg-Ca porogen removal (2 h in EDTA/disodium citrate) on day 7, and group 3 received both Alg-Ca and GMHA porogen removal by EDTA treatment at day 7 followed by hyaluronidase (3 h) treatment on day 14. To enhance cell viability, the solutions of EDTA/disodium citrate and hyaluronidase were prepared in DMEM. After each treatment, all samples were rinsed in fresh culture medium for 15 min for five times to remove the stimuli reagents and dissociated porogen components.

2.7.4. Cell proliferation and morphology

On day 1, 8, 15 and 21, a slice (0.2 mm thick) was collected from the center of scaffolds from each group for live/Dead staining (Invitrogen) following manufacture's protocol. On day 21, scaffolds from each group were fixed in 4% paraformaldehyde overnight and stored in 70% ethanol at 4 °C until processed. Scaffolds were then embedded in paraffin and cell morphology was examined using H&E staining. For immunostaining, enzymatic antigen retrieval was performed using 0.1% trypsin at 37 °C for 15 min, followed by blocking buffer treatment consisting of 2% goat serum, 3% BSA and 0.1% Triton X-100 in 1XPBS. Sections were then incubated in rabbit polyclonal antibody to collagen type II and X (Abcam) overnight at 4 °C and secondary antibody (Alexa Fluor 488 goat anti-rabbit, Invitrogen) incubation for an hour at room temperature. Nuclei were counterstained with DAPI mounting medium (Vectashield) and images were taken with a Zeiss fluorescence microscope. Sections were also stained with all reagents without primary antibody for negative controls. Cell density and collagen deposition were quantified by calculating the average fluorescence intensity per pixel using open-source program ImageJ.

2.8. Statistics

All quantitative data were expressed as mean ± standard error and were verified by analysis of variance using student T-Test with equal variance. P values (two-tails) of less than 0.05 were considered statistically significant, and p values less than 0.005 were considered statistically highly significant.

3. Results

3.1. Stimuli-responsive pore-formation in mono-porogen scaffolds

Three types of stimuli-responsive porogens were fabricated based on type-A gelatin (Gel-A), methacrylated hyaluronic acid and alginate (Fig. 2A–C). When suspended in PBS, the diameter of the

Please cite this article in press as: Han L-H, et al., Dynamic tissue engineering scaffolds with stimuli-responsive macroporosity formation, Biomaterials (2013), http://dx.doi.org/10.1016/j.biomaterials.2013.02.051

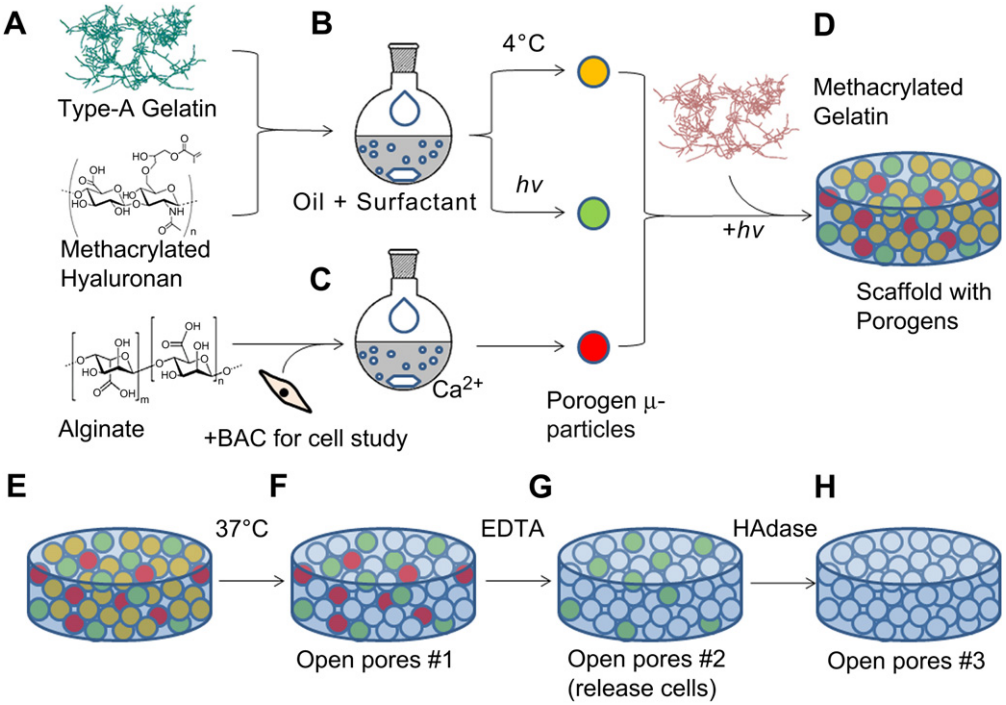

Fig. 2. (A–C) Experimental scheme for fabricating three types of stimuli-responsive porogens; (D) Co-encapsulating three types of porogens into photocrosslinkable gelatin hydrogels; (E) Step-wise macropore formation in gelatin hydrogels using stimuli specific for each porogen removal.

porogen beads range about 150–250 μm for GelA porogen, 200–300 μm for Alg-Ca porogen, and 100–200 μm for GMHA porogen. Upon mixing with 20% GelB-MA solution, the size of GelA and GMHA porogens remained roughly the same while the Alg-Ca porogen microparticles shrank down to 50–100 μm. Upon exposure to corresponding individual stimulus, hydrogel scaffolds with mono-porogen formed macroporosity as shown by the fluorescence imaging and scanning electron microscopy (Fig. 3). Such macropores were highly interconnected and resembled the shapes of porogen microparticles. The GelA porogens resulted in smooth internal surfaces with micron-scaled mesh (Fig. 3A–B), and such microporosity was also observed in GelB hydrogels containing no porogen (not shown). In contrast to GelA porogen, Alg-Ca and GMHA porogens produced macropores with granulated and fibrous microstructures (Fig. 3C–F).

3.2. Sequential macropore formation in tri-porogen scaffolds

To examine the efficacy of dynamic macropore formation, tri-porogen scaffolds were prepared (Fig. 2D) and treated by the stimuli in a sequential manner (Fig. 2E–H): incubation in 37 °C PBS overnight, incubation in Ethylenediamine tetraacetic acid (EDTA)/

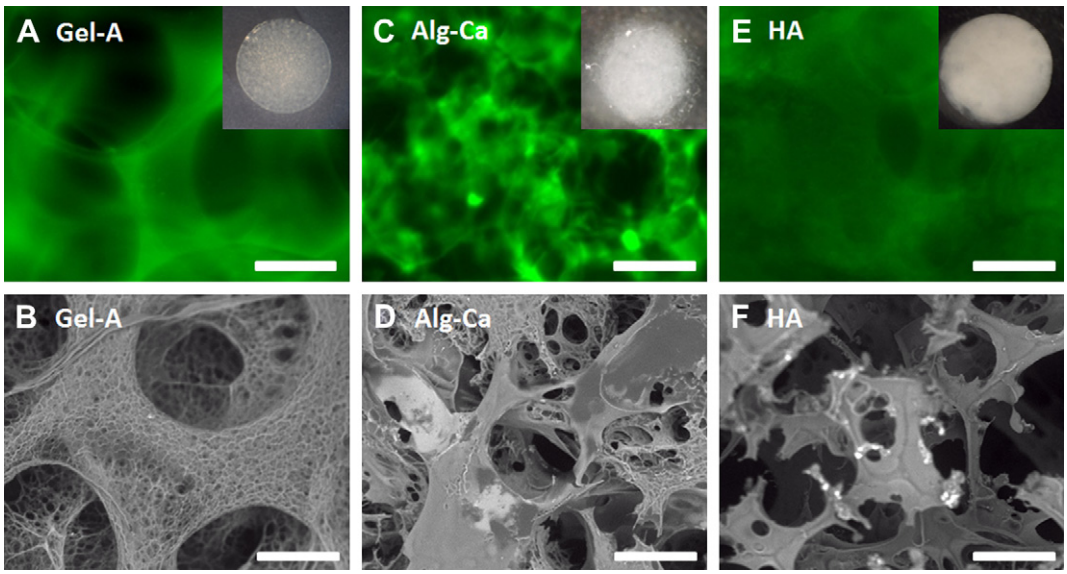

Fig. 3. Morphology of mono-porogen containing scaffold after porogen removal as shown by fluorescence imaging and scanning electron microscopy. Scaffold morphology after the removal of porogens based on type A gelatin (Gel-A) (A, B); alginate-calcium (Alg-Ca) (C, D) and hyaluronic acid (HA) (E, F). Scale bars: 100 μm.

Please cite this article in press as: Han L-H, et al., Dynamic tissue engineering scaffolds with stimuli-responsive macroporosity formation, Biomaterials (2013), http://dx.doi.org/10.1016/j.biomaterials.2013.02.051

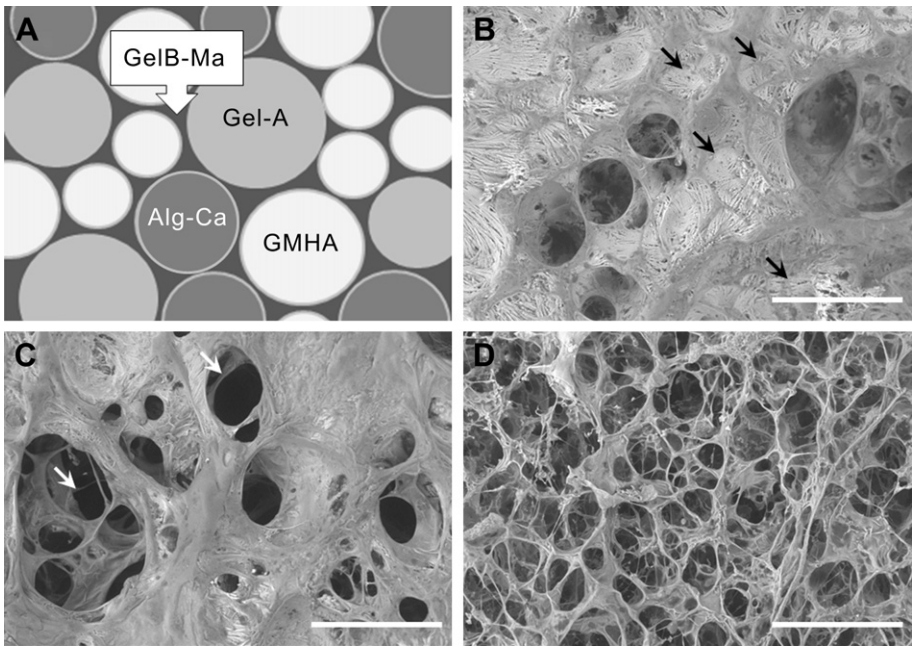

Fig. 4. Scanning electron microscopy of tri-porogen-based scaffolds upon sequential porogen removal: (A) Illustration; (B) Type A gelatin porogen was removed by 37 °C incubation; (C) Alginate-calcium porogen was removed by EDTA/disodium citrate; and (D) Hyaluronic acid porogen was removed by hyaluronidase. Scale bars: 200 μm.

disodium citrate solution for 2 h, and incubation in 37 °C hyaluronidase (HAdase) solution for 3 h.

Treating tri-porogen scaffolds by a series of stimuli led to sequential macropore formation (Fig. 4). Macropores began to emerge from the scaffold upon the removal of GelA porogen by temperature change (25–37 °C) (Fig. 4B). The macroporosity level at this stage was low and the pores were only slightly interconnected, as most of scaffold volume was still occupied by the Alg-Ca and GMHA porogens. Upon EDTA treatment, the macroporosity increased markedly with the dissolution of Alg-Ca porogens

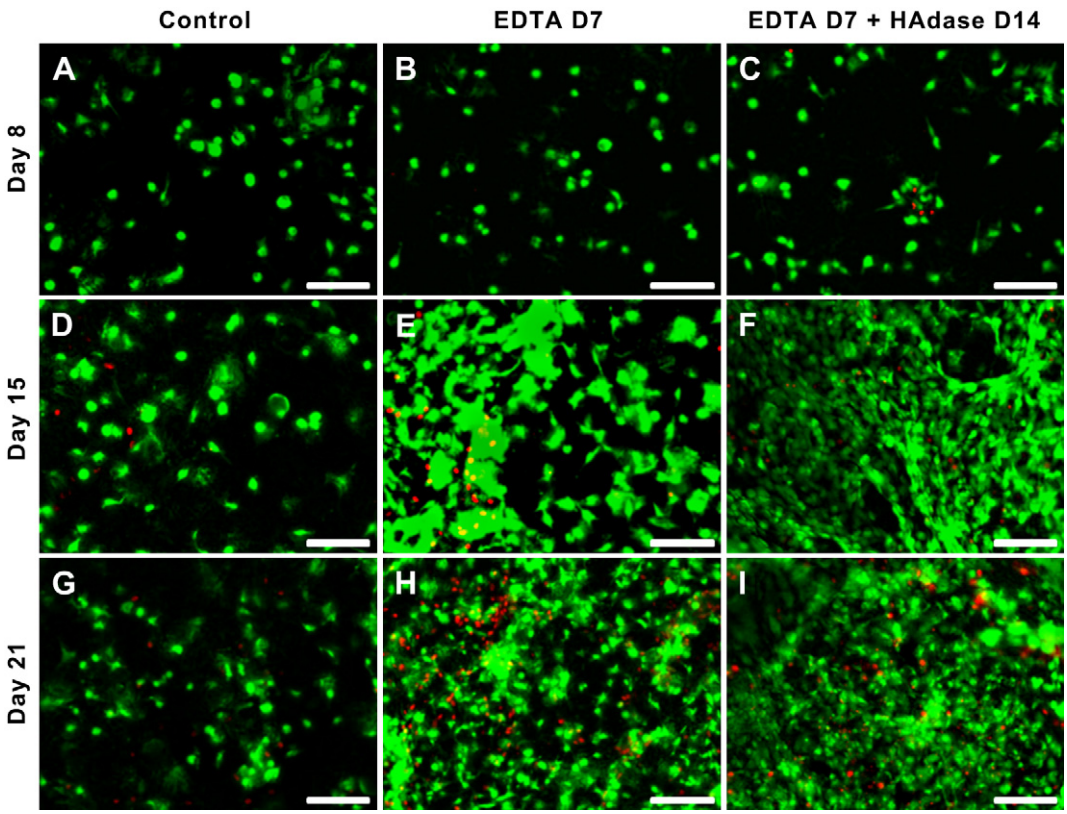

Fig. 5. Cell viability and morphology in hydrogels containing three types of porogens over 21 days. Three groups were examined including single porogen removal (control), dual porogen removal (EDTA D7) and tri-porogen removal (EDTA D7 + HAdase D14). Scale bars: 100 μm.

Please cite this article in press as: Han L-H, et al., Dynamic tissue engineering scaffolds with stimuli-responsive macroporosity formation, Biomaterials (2013), http://dx.doi.org/10.1016/j.biomaterials.2013.02.051

(Fig. 4C). HAdase treatment led to further increase in porosity with the removal of GMHA porogens (Fig. 4D), which formed highly macroporous scaffold with great interconnectivity.

3.3. Cell proliferation and ECM production in tri-porogen scaffolds

3.3.1. Effects of sequential macropore formation on cell proliferation

To examine the effect of dynamic macropore formation to 3D cell culture, the aforementioned tri-porogen scaffolds were prepared with BACs laden Alg-Ca porogen, and treated by the stimuli. Compared to the control scaffold without exposure to EDTA and HAdase, sequential treatments (EDTA on day 7 and HAdase on day 14) led to much higher BAC proliferation over three weeks (Fig. 5). On day 1, the BACs from all groups were still in the Alg-Ca porogen and maintained spherical morphology (not shown). On day 8, slight cell spreading started to emerge in all groups (Fig. 5A–C). By day 15, the two groups treated by EDTA (Fig. 5E, F) showed extensive cell spreading and dramatically enhanced cell density close to confluence, whereas minimal cell spreading and growth was observed in the control group (non-treated) (Fig. 5D). Similar trend was observed in all groups by day 21 (Fig. 5G–I).

3.3.2. Effects of sequential macropore formation on extracellular matrix (ECM) deposition

H&E staining and immunofluorescence staining were performed to examine cell and ECM morphology at day 21 (Fig. 6). Compared to the control group, groups treated with EDTA on day 7 performed higher cell density and more extensive ECM deposition. Group receiving further HAdase treatment at Day 14 showed further increase in cell density and ECM production, with extensive amount of type II and type X collagen deposited throughput the scaffold.

Quantifications based on the immunostaining showed that the increase in cell density and ECM production in response to dynamic pore-formation was statistically significant (Fig. 7A–C). By day 21, the cell density in the two groups treated with EDTA was comparable and 1.5 fold higher than the non-treated group ($p < 0.005$) (Fig. 7A). Groups treated with EDTA showed 31% more type II collagen compared to the control group ($p < 0.05$), and EDTA + HAdase led to further increased collagen II deposition (95%) (Fig. 7B). Similarly, these two groups showed ~1–2 fold higher type X collagen deposition compared to the control ($p < 0.001$) (Fig. 7C). Tri-porogen removal (EDTA + HAdase) led to higher amount of collagen deposition compared to the group treated with dual porogens removal (EDTA), but the difference was not statistically significant.

4. Discussion

Here we report the development of a platform for introducing dynamic macroporosity in cell-laden hydrogels using stimuli-responsive porogens. Sequential exposure to multiple stimuli (temperature, small chelating molecules, and enzyme) led to gradual formation of interconnected macropores throughout 3D

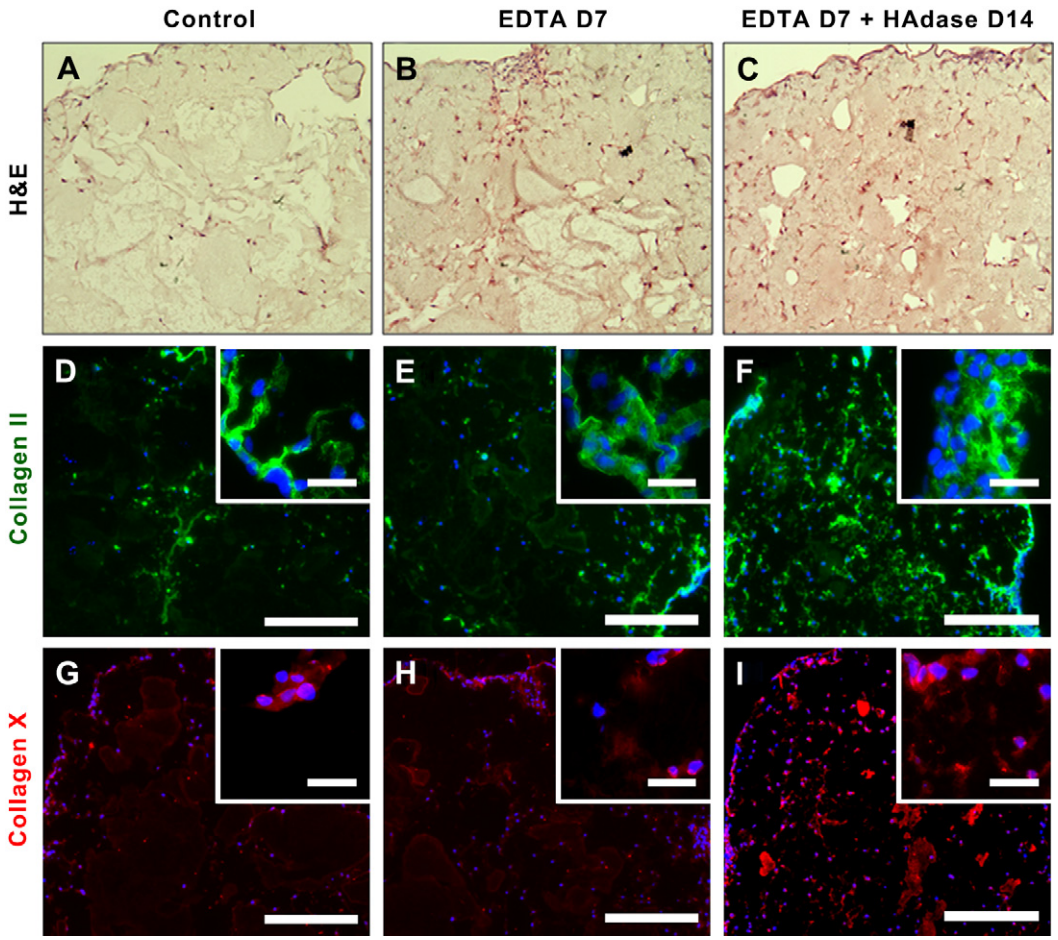

Fig. 6. Histology of chondrocyte-laden hydrogels containing three types of porogens by day 21. (A–C) H&E staining, (D–F) immunofluorescence staining of type II collagen, and (G-I) type-X collagen. Scale bars: 100 μm (Inset: 15 μm).

Please cite this article in press as: Han L-H, et al., Dynamic tissue engineering scaffolds with stimuli-responsive macroporosity formation, Biomaterials (2013), http://dx.doi.org/10.1016/j.biomaterials.2013.02.051

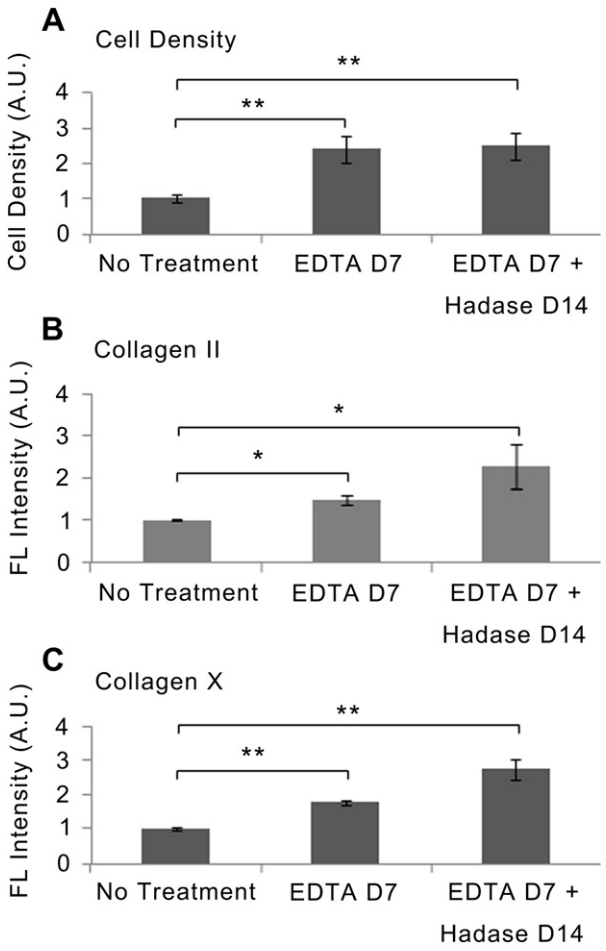

Fig. 7. Quantified cell density and matrix deposition in chondrocyte-laden hydrogels based on immunofluorescence staining. (A) Cell density; (B) Amount of Type-II collagen; (C) Amount of type-X collagen. (Error bars: standard deviation; *: $p < 0.005$; **: $p < 0.001$).

scaffolds. We have chosen biomaterials commonly used for tissue engineering applications (gelatin, alginate, and hyaluronic acid) to fabricate the porogens, and the process is non-cytotoxic. Sequential porogen removal led to the significantly enhanced cell proliferation and ECM production compared to the control scaffold with fixed macroporosity. Our data also demonstrated that such porogens may also be used as cell-delivery vehicles for temporal cell release in 3D scaffold. The macropores created by porogen removal are highly interconnected and the size of macropores can be tuned by modulating the diameter of porogens. We have created macropores about one order of magnitude larger than the size of cells, which can be advantageous for tissue formation by facilitating vascularization, cell proliferation, and production of ECM components. The surface topography of macropores can be further tuned by the porogen material of choice, which may be a result of charge interactions between the different polymers (Fig. 3D–F). Given that topographical cues also play an important role in regulating cell behavior, choosing porogens materials that produce desirable topographical cues may also be exploited to promote cell behavior that is sensitive to the micro- or nano-structures in hydrogels [30–33].

To examine the effects of dynamic pore-formation on cell proliferation and ECM deposition in 3D, we have chosen neonatal bovine chondrocytes as a model cell type and encapsulated chondrocytes in Alg-Ca porogens, followed by mixing with two other porogens to form a tri-porogen based scaffold. Prior to the exposure of EDTA, the BACs maintained its density and morphology, suggesting that BACs remained trapped in Alg-Ca porogens. Following EDTA exposure at day 7, Alg-Ca porogen was dissolved and the chondrocytes proliferated and reached confluency within a week. In contrast, chondrocytes in the control group without EDTA exposure showed minimal cell proliferation and spreading throughout the culture period. The ECM production by the chondrocytes (type II and type X collagen) was significantly enhanced by Alg-Ca porogen removal, and was further enhanced by 50% with additional GMHA porogen removal (Fig. 7A, B). Given that higher collagen deposition correlated with BAC aggregation (insets of Fig. 6D–I), the enhanced production of type II and type X collagen may be contributed by the increased level of cell–cell contact following GMHA porogen removal (Fig. 5). Removing Alg-Ca porogen alone led to enhanced cell proliferation and spreading, which reached confluence by day 15 (Figs. 5 and 7). Together, these results demonstrate several advantages of the platform developed herein in comparison with previously reported macropore-forming methods. First, dynamic pore-formation allows the temporal control of cell-releasing and the pace of cell proliferation and ECM production, which can be applied to promoting desired cell processes at different stages of tissue development. Recently, several groups have demonstrated co-encapsulating cells and non-cytotoxic porogens for macropore formation in situ [18,19], but these methods do not allow controlled cell-releasing nor dynamic pore-formation. Second, our process is non-cytotoxic and allows more homogeneous cell distribution, which is important to mediate cell viability and the tissue-forming efficiency in 3D.

One challenge associated with porogens removal is the potential decrease in scaffold mechanical property, which will be particularly important for engineering weight-bearing tissues such as bone and cartilage. This may be overcome by controlling the timing of stimuli exposure for pore-formation in accordance with the pace of cell proliferation and ECM production, such that the decrease in scaffold mechanical strength can be compensated by the newly formed tissues [34]. An alternative strategy is to incorporating fibrous materials [35], such as PLGA microfibers in the scaffold, which may enhance scaffold rigidity. While here we demonstrated an example using hydrogel-based scaffolds, such dynamic pore-formation strategy may also be combined with other scaffolds, in which the mechanical property can be dominated by the mechanical strength of the scaffold of choice, and the dissolution of stimuli-responsive porogens may not cause significant changes in the bulk mechanical property.

Using gelatin, Alg-Ca, and GMHA as model porogens, here we demonstrated the concept of dynamic macropore formation as well as the potential of controlling macroporosity in a temporal manner to facilitate cell proliferation and tissue formation. This platform may be further extended by exploiting other materials as porogens that can be degraded using different stimuli such as hydrolysis, MMP-sensitive peptides [36] or photo-degradation [22].

5. Conclusion

In summary, here we report a process to create 3D hydrogels with dynamically tunable macroporosity using stimuli-responsive porogens including type-A gelatin, alginate and hyaluronic acid. Upon exposure to specific stimuli at multiple time points, highly interconnected macropore formation was observed throughout the 3D hydrogels and such stimuli-responsive porogens can also serve as cell-delivery vehicles for temporal cell release within 3D scaffolds. Our results showed effective cell release from Alg porogen with high cell viability, and sequential macropore formation led to markedly increased cell proliferation and extracellular matrix production by chondrocytes throughout the 3D scaffolds. The platform reported herein provides a valuable tool to create dynamic

Please cite this article in press as: Han L-H, et al., Dynamic tissue engineering scaffolds with stimuli-responsive macroporosity formation, Biomaterials (2013), http://dx.doi.org/10.1016/j.biomaterials.2013.02.051

tissue engineering scaffolds to facilitate desirable cellular fate processes and tissue formation in a stimuli-responsive manner. It may also be utilized as a valuable in vitro model for fundamental studies to examine cell responses to dynamic niche properties such as loss of biochemical or physical cues, which is often found in various diseases progression processes.

Competing financial interests

This work has been disclosed to the Office Technology Licensing at Stanford University.

Acknowledgments

The authors would like to thank the McCormick Faculty Award, March of Dimes Foundation and Stanford Bio-X Interdisciplinary Initiative grant for funding.

References

[1] Cukierman E, Pankov R, Stevens DR, Yamada KM. Taking cell-matrix adhesions to the third dimension. Science 2001;294(5547):1708–12.
[2] Abbott A. Cell culture: biology's new dimension. Nature 2003;424(6951):870–2.
[3] Debnath J, Mills KR, Collins NL, Reginato MJ, Muthuswamy SK, Brugge JS. The role of apoptosis in creating and maintaining luminal space within normal and oncogene-expressing mammary acini. Cell 2002;111(1):29–40.
[4] Mosiewicz KA, Johnsson K, Lutolf MP. Phosphopantetheinyl transferase-catalyzed formation of bioactive hydrogels for tissue engineering. J Am Chem Soc 2010;132(17):5972–4.
[5] DeForest CA, Polizzotti BD, Anseth KS. Sequential click reactions for synthesizing and patterning three-dimensional cell microenvironments. Nat Mater 2009;8(8):659–64.
[6] Flaim CJ, Chien S, Bhatia SN. An extracellular matrix microarray for probing cellular differentiation. Nat Methods 2005;2(2):119–25.
[7] Ross AM, Jiang Z, Bastmeyer M, Lahann J. Physical aspects of cell culture substrates: topography, roughness, and elasticity. Small 2012;8(3):336–55.
[8] Fierz FC, Beckmann F, Huser M, Irsen SH, Leukers B, Witte F, et al. The morphology of anisotropic 3D-printed hydroxyapatite scaffolds. Biomaterials 2008;29(28):3799–806.
[9] Gauvin R, Chen YC, Lee JW, Soman P, Zorlutuna P, Nichol JW, et al. Microfabrication of complex porous tissue engineering scaffolds using 3D projection stereolithography. Biomaterials 2012;33(15):3824–34.
[10] Fozdar DY, Soman P, Lee JW, Han LH, Chen S. Three-dimensional polymer constructs exhibiting a tunable negative Poisson's ratio. Adv Funct Mater 2011;21(14):2712–20.
[11] Ovsianikov A, Schlie S, Ngezahayo A, Haverich A, Chichkov BN. Two-photon polymerization technique for microfabrication of CAD-designed 3D scaffolds from commercially available photosensitive materials. J Tissue Eng Regen Med 2007;1(6):443–9.
[12] Xiao J, Duan H, Liu Z, Wu Z, Lan Y, Zhang W, et al. Construction of the recellularized corneal stroma using porous acellular corneal scaffold. Biomaterials 2011;32(29):6962–71.
[13] Choi SW, Yeh YC, Zhang Y, Sung HW, Xia Y. Uniform beads with controllable pore sizes for biomedical applications. Small 2010;6(14):1492–8.
[14] Salerno A, Guarnieri D, Iannone M, Zeppetelli S, Netti PA. Effect of micro- and macroporosity of bone tissue three-dimensional-poly(epsilon-caprolactone) scaffold on human mesenchymal stem cells invasion, proliferation, and differentiation in vitro. Tissue Eng Part A 2010;16(8):2661–73.
[15] Hong Y, Guan J, Fujimoto KL, Hashizume R, Pelinescu AL, Wagner WR. Tailoring the degradation kinetics of poly(ester carbonate urethane)urea thermoplastic elastomers for tissue engineering scaffolds. Biomaterials 2010;31(15):4249–58.
[16] Mondrinos MJ, Dembzynski R, Lu L, Byrapogu VK, Wootton DM, Lelkes PI, et al. Porogen-based solid freeform fabrication of polycaprolactone-calcium phosphate scaffolds for tissue engineering. Biomaterials 2006;27(25):4399–408.
[17] Chen VJ, Ma PX. Nano-fibrous poly(L-lactic acid) scaffolds with interconnected spherical macropores. Biomaterials 2004;25(11):2065–73.
[18] Hwang CM, Sant S, Masaeli M, Kachouie NN, Zamanian B, Lee SH, et al. Fabrication of three-dimensional porous cell-laden hydrogel for tissue engineering. Biofabrication 2010;2(3):035003.
[19] Scott EA, Nichols MD, Kuntz-Willits R, Elbert DL. Modular scaffolds assembled around living cells using poly(ethylene glycol) microspheres with macroporation via a non-cytotoxic porogen. Acta Biomater 2010;6(1):29–38.
[20] Lyons FG, Al-Munajjed AA, Kieran SM, Toner ME, Murphy CM, Duffy GP, et al. The healing of bony defects by cell-free collagen-based scaffolds compared to stem cell-seeded tissue engineered constructs. Biomaterials 2010;31(35):9232–43.
[21] Hollister SJ. Porous scaffold design for tissue engineering. Nat Mater 2005;4(7):518–24.
[22] Lutolf MP, Lauer-Fields JL, Schmoekel HG, Metters AT, Weber FE, Fields GB, et al. Synthetic matrix metalloproteinase-sensitive hydrogels for the conduction of tissue regeneration: engineering cell-invasion characteristics. Proc Natl Acad Sci U S A 2003;100(9):5413–8.
[23] Kraehenbuehl TP, Ferreira LS, Zammaretti P, Hubbell JA, Langer R. Cell-responsive hydrogel for encapsulation of vascular cells. Biomaterials 2009;30(26):4318–24.
[24] Moss JA, Stokols S, Hixon MS, Ashley FT, Chang JY, Janda KD. Solid-phase synthesis and kinetic characterization of fluorogenic enzyme-degradable hydrogel cross-linkers. Biomacromolecules 2006;7(4):1011–6.
[25] Nichol JW, Koshy ST, Bae H, Hwang CM, Yamanlar S, Khademhosseini A. Cell-laden microengineered gelatin methacrylate hydrogels. Biomaterials 2010;31(21):5536–44.
[26] Khalil S, Sun W. Bioprinting endothelial cells with alginate for 3D tissue constructs. J Biomech Eng 2009;131(11):111002.
[27] Burdick JA, Chung C, Jia X, Randolph MA, Langer R. Controlled degradation and mechanical behavior of photopolymerized hyaluronic acid networks. Biomacromolecules 2005;6(1):386–91.
[28] Suri S, Schmidt CE. Cell-laden hydrogel constructs of hyaluronic acid, collagen, and laminin for neural tissue engineering. Tissue Eng Part A 2010;16(5):1703–16.
[29] Maksimenko AV, Schechilina YV, Tischenko EG. Role of the glycosaminoglycan microenvironment of hyaluronidase in regulation of its endoglycosidase activity. Biochemistry (Mosc) 2003;68(8):862–8.
[30] Raines AL, Olivares-Navarrete R, Wieland M, Cochran DL, Schwartz Z, Boyan BD. Regulation of angiogenesis during osseointegration by titanium surface microstructure and energy. Biomaterials 2010;31(18):4909–17.
[31] Kumar G, Waters MS, Farooque TM, Young MF, Simon Jr CG. Freeform fabricated scaffolds with roughened struts that enhance both stem cell proliferation and differentiation by controlling cell shape. Biomaterials 2012;33(16):4022–30.
[32] Watari S, Hayashi K, Wood JA, Russell P, Nealey PF, Murphy CJ, et al. Modulation of osteogenic differentiation in hMSCs cells by submicron topographically-patterned ridges and grooves. Biomaterials 2012;33(1):128–36.
[33] Chan LY, Birch WR, Yim EK, Choo AB. Temporal application of topography to increase the rate of neural differentiation from human pluripotent stem cells. Biomaterials 2013;34(2):382–92.
[34] Sampat SR, O'Connell GD, Fong JV, Alegre-Aguaron E, Ateshian GA, Hung CT. Growth factor priming of synovium-derived stem cells for cartilage tissue engineering. Tissue Eng Part A 2011;17(17–18):2259–65.
[35] Huttunen M, Kellomaki M. A simple and high production rate manufacturing method for submicron polymer fibres. J Tissue Eng Regen Med 2011;5(8):e239–43.
[36] Anderson SB, Lin CC, Kuntzler DV, Anseth KS. The performance of human mesenchymal stem cells encapsulated in cell-degradable polymer-peptide hydrogels. Biomaterials 2011;32(14):3564–74.

Please cite this article in press as: Han L-H, et al., Dynamic tissue engineering scaffolds with stimuli-responsive macroporosity formation, Biomaterials (2013), http://dx.doi.org/10.1016/j.biomaterials.2013.02.051